Resveratrol Trisepoxy-Based High-Performance Resin Formulation and Carbon Fiber-Reinforced Composite Processing for Structural Applications

Dyer, William E.; Alasoo, Elmar Daniel; Lorenz, Niklas; Kumru, Baris

DOI
10.1021/acsomega.5c05906

Publication date
2025

Document Version
Final published version

Published in
ACS Omega

ACS OMEGA

Open Access

http://pubs.acs.org/journal/acsodf

Article

Resveratrol Trisepoxy-Based High-Performance Resin Formulation and Carbon Fiber-Reinforced Composite Processing for Structural Applications

William E. Dyer,[†] Elmar-Daniel Alasoo,[†] Niklas Lorenz, and Baris Kumru*

Cite This: *ACS Omega* 2025, 10, 49887−49895

Read Online

ACCESS | Metrics & More | Article Recommendations | Supporting Information

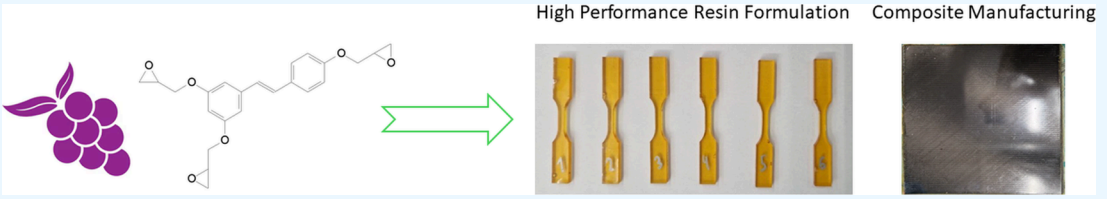

ABSTRACT: Tactix 742 (a trifunctional aromatic epoxy resin) is a benchmark epoxy monomer elucidating the highest T_g epoxy resin system; however, its manufacturing relies on petroleum-based toxic chemistries. In the realm of sustainability, potential replacement of Tactix 742 with a renewable platform possessing similar thermomechanical properties as well as processing character is critical. The resin system of renewable resveratrol triglycidyl ether with aerograde hardener 4,4-diaminodiphenylsulfone shows an ultrahigh T_g of 324 °C and mechanical properties comparable to the industrially used petro-based tris(hydroxyl phenyl)methane epoxy monomer. The results highlight the untapped potential that biobased molecules show in innovating existing high-performance plastic formulations while potentially increasing sustainability potential in the future. Resveratrol triglycidyl ether-4,4-diphenyldisulfone (RTE-DDS) formulation shows T_g, stiffness, strength, and processing behavior similar to that of the industrially used petro-equivalent formulation (T742-DDS) with slightly lower modulus and strength in both tensile and flexural testing. Fracture toughness of the biobased formulation is 61% higher than the petro-based formulation. CFRP manufacturing yields high-quality composite materials tested in compression, interlaminar shear, and in-plane shear modes. Fiber volume content is slightly lower than ideal due to the formulations high viscosity and the choice of vacuum bagging and autoclave manufacturing technique, but low void content of 0.55% ± 0.26 allows for accurate characterization of CFRP laminates. Conclusions are drawn regarding the future potential of resveratrol epoxy monomer in high-performance epoxy CFRPs.

INTRODUCTION

Epoxy resins are the most abundant class of thermoset plastics due to their desirable material properties and versatile processability, which can be tailored by choice of the particular monomers and curing agents.[1] These curing agents are typically amines, phenolics, anhydrides, or thiols depending on the specific application and processing requirements.[2] Alongside attractive properties such as adhesive strength (due to hydroxyl formation upon ring opening), chemical resistance, stiffness, strength, low-brittleness (compared to other thermoset types), and well-established synthetic routes, the sheer versatility in epoxy-hardener combinations leads to the possibility to process epoxies across a considerable range of temperature, time, and viscosity requirements.[3] Indeed epoxy resin formulations are found throughout the economy: from simple household adhesives, all the way to the matrix material in aerospace structural CFRPs.[4−7] While the underlying chemical reactions occurring are the same across formulations, the structure of the epoxy monomer and hardener greatly affects reactivity, processing, and the resulting material's thermal and mechanical properties.[1]

Since their discovery and patent almost 90 years ago,[8] epoxy−amine resin formulations have risen to become a ubiquitous epoxy resin.[1] Epoxy monomers find use across the domains of electrical insulation, adhesives, coatings, composites, and castings, epoxy-amine formulations included; however, they find particular use in composite materials. This is due to a few unique properties of the epoxy−amine interactions. First, the epoxy−amine reaction produces a densely cross-linked network due to each amine hydrogen reacting with one epoxy group.[9−11] Second, hydrogen bonding between the nitrogen lone pair, on top of the hydroxyl groups present in other classes of formulations,[12,13] leads to stronger intermolecular interactions, giving rise to higher stiffness[14] and

Received: June 23, 2025
Revised: September 14, 2025
Accepted: September 22, 2025
Published: October 15, 2025

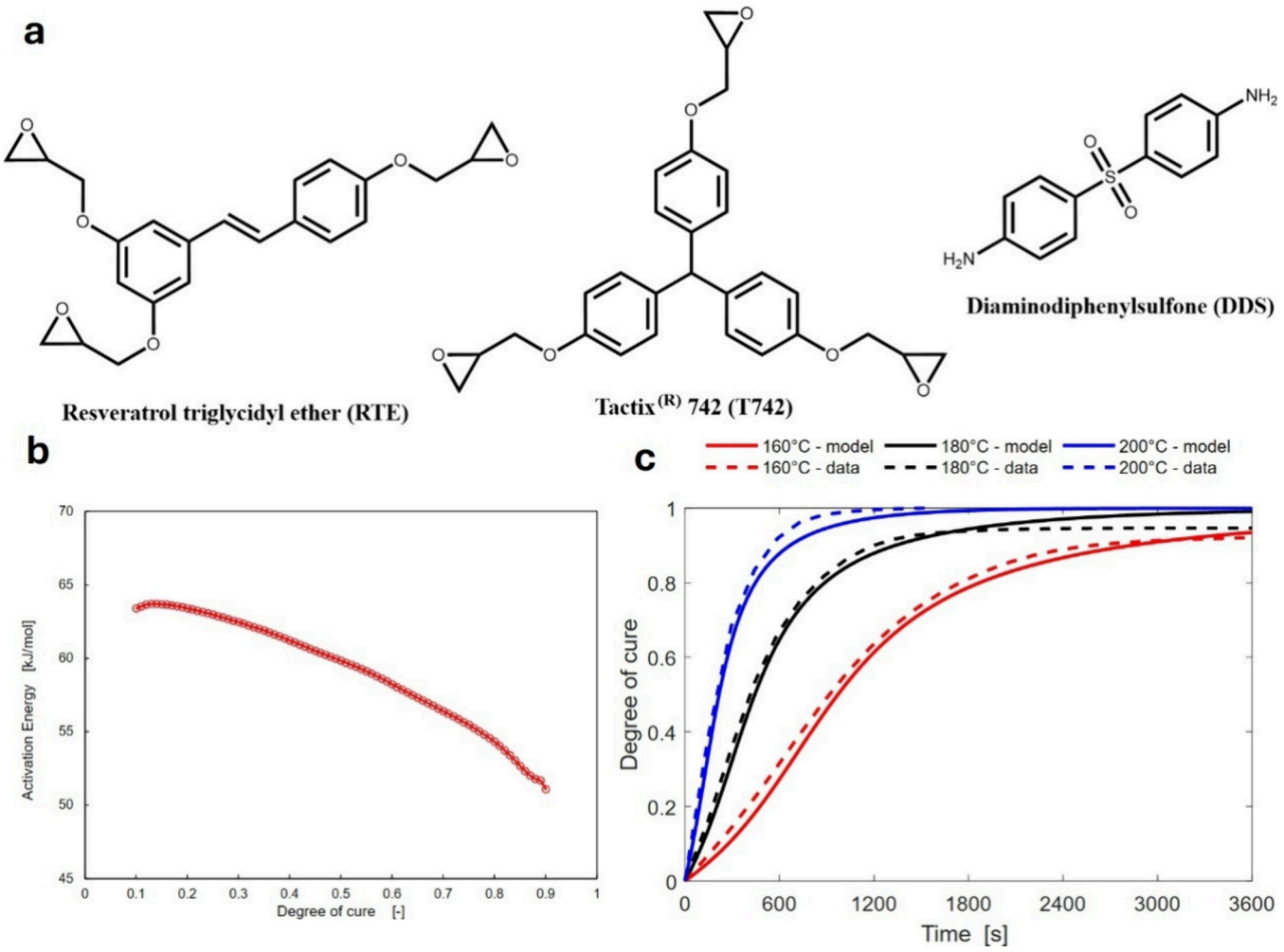

Figure 1. (a) Chemical structures of monomers used in this work. (b) E_ξ-dependency for the different resin formulations derived by the Friedman method. (c) Comparison of measurements for isothermal curing.

better adhesive properties, which is essential in composite materials.[15] These two factors also contribute to better thermal resistance compared to other epoxy formulations.[1] Industry formulations are tailored for specific processing and reactivity requirements, and the vast array of monomers and hardeners available gives great breadth in the manufacturing choice of composite materials.[16] The wide range of formulations available have given rise to further innovation within the manufacturing domain, with high-output molding techniques such as RTM pioneering and giving rise to complex, more sustainable production of high-performance CFRP materials for use in automotive and aerospace industries.[17,18] These pioneering manufacturing techniques continue to drive innovation within the composites industry and rely heavily on the versatility of epoxy−amine formulations.[19]

While the established epoxy−amine formulations have been refined and adjusted over the years to yield reliable products, there is always scope for innovative formulations to enter the market and disrupt the status-quo. Alongside this pressure to innovate, the plastics industry has been facing societal pressure on a much larger scale than previous decades, and this of course comes from the need to increase sustainability in all aspects of human civilization.[20,21] Cleaner energy, lower reliance on fossil fuels (greater resiliency), reducing plastic pollution, and more eco-friendly and less-toxic products are the main areas of scrutiny.[22] As a result, the research domain of sustainable polymers has seen huge growth in the last 2 decades, with efforts focusing on both ends of the linear lifecycle of plastic products.[23] Research papers focusing on the use of biobased materials are abundant, with academia and industry alike lauding the potential for more sustainable "drop-in" products—that is, products that can easily fit into current manufacturing processes.[24]

Biobased chemical building blocks for sustainable plastics production are a large research field in the domains of synthetic and industrial chemistry.[25] There are hundreds of contenders to replace current petrochemicals, which is important in meeting the sustainability requirements for all industries as each application requires unique biomaterial properties.[26,27] The most accessible and economically competitive materials are those generated from plant waste, which contains many sugars and polymers including cellulose, hemicellulose, and lignin.[28] These three components are found to varying degrees depending on the plant feedstock, and the properties of the monomers extracted and bioplastics produced from each component differ greatly. Cellulose, hemicellulose, and smaller sugars contain large amounts of oxygen atoms, whereas lignin contains large amounts of aromatic phenyl groups. Aromatics are of particular interest in higher-performance applications as they impart high T_g and good

https://doi.org/10.1021/acsomega.5c05906
ACS Omega 2025, 10, 49887−49895

thermal resistance, stiffness, and strength to plastics.[29] The aromatics extracted from plant material contain heteroatoms, most often oxygen in the form of alcohol, aldehyde, or ether moieties. This is of great significance when considering the suitability of a molecule for its use in bioplastics as the synthesis of epoxy monomers is currently based on epichlorohydrin, itself a potentially biobased molecule from glycerol.[30] Therefore, we seek multifunctional phenolic compounds when looking for biobased epoxies for high-performance applications.

Many such phenolics have been isolated directly or indirectly from lignin including eugenol,[31] vanillin,[32,33] daidzein,[34] resorcinol,[35] gallic acid,[36] and resveratrol.[37] The wide variety of bioderived chemicals being explored is essential in meeting the variety of applications for which aromatic molecules are used within the plastics industry, which includes advanced applications such as aerospace.[38,39] Furthermore, other biosynthetic techniques are being explored for the production of industrial chemicals, including fermentation and bacterial and enzymatic syntheses.[30,40−42] The majority of articles investigating biobased epoxy−amine formulations focus largely in the chemistry domain, with many papers investigating synthetic routes to produce potential biobased alternatives.[40,43−46] Initial characterization is often given but usually lacks more systematized testing (such as the use of ASTM standards) to gauge mechanical performance. More research is needed in bridging the gap between chemistry and engineering literature, enabling trialling and future adoption of these potentially more sustainable resins. This includes thoroughly characterizing the curing behavior of novel biobased resin formulations following established procedures and exploring composite manufacturing to reveal specific macroscopic mechanical characteristics and quantitatively assess the potential of the novel biobased resin formulation.[26,47,48] Systematized testing also increases confidence in claims that biobased plastics can compete with existing petro-based formulations, specifically at the high-performance level.

Resveratrol formulations in particular have been shown to exhibit attractive thermal properties including high T_g, high char yields, and maintained modulus at elevated temperatures.[49−52] The first research paper using resveratrol in an epoxy resin system appears in 2018, yielding a resin with T_g of 148 °C and good heat resistance compared against the ubiquitous bisphenol A epoxy (BADGE).[53] In 2020, the resveratrol epoxy was again compared against BADGE using an anhydride curing agent and found similarly promising results including adequate mechanical properties, high char yield, and low permittivity with relevance to electronic applications.[51] Following this, many more studies aim to elucidate the properties of resveratrol-based thermosetting resins including chemical modification to tailor properties of materials.[52,54,55]

The following study builds upon this literature by providing in-depth curing analysis of the RTE-DDS formulation, resin comparison against tris(hydroxyl phenyl)methane epoxy (Tactix 742) monomer, and high-quality CFRP manufacturing and testing of resveratrol-based epoxy−amine formulation. The comparison resin is typically used in structural adhesive and composite formulations, especially in high-heat zone applications. ASTM procedures are followed, allowing for a fair and comprehensive comparison of these two resin systems.

RESULTS AND DISCUSSION

Curing Kinetics. Chemical structures of the monomers are provided in Figure 1a. Curing kinetics were investigated using dynamic and isothermal heating experiments via a DSC. We utilized model-free and model-based procedures to gain a more in-depth understanding of the curing behavior of RTE-DDS. Initial studies revealed a high T_g; therefore, the curing cycle was selected as 180 °C for 2 h and 220 °C for 1 h postcure. This high postcuring temperature ensures a high level of cross-linking and maximization of mechanical properties without being excessively high (to promote epoxy ring opening via hydroxyl groups or network degradation).

Model-Free Kinetics. Various analytical and computational methods have been applied to approximate the data derived from dynamic or isothermal DSC measurements into an appropriate mathematical expression. The isoconversional principle states that the reaction rate $\frac{d\xi}{dt}$ at a certain isoconversional value ξ ($0 \leq \xi \leq 1$) solely depends on the temperature (eq 1):[56,57]

$$\left[\frac{\partial \ln\left(\frac{d\xi}{dt}\right)}{\partial T^{-1}}\right]_{\xi} = -\frac{E_\xi}{R} \tag{1}$$

whereas E_ξ is the apparent activation energy for a certain degree of cure ξ, and R is the universal gas constant. Based on eq 1, a model-free value of the apparent activation energy can be estimated for each ξ value. Within the present work, we utilize the Freedman's method[58] given in the following eq 2:

$$\ln\left(\frac{d\xi}{dt}\right)_{\xi,i} = \ln[A_\xi f(\xi)] - \frac{E_\xi}{RT_{\xi,i}} \tag{2}$$

Applying this method requires knowledge of the reaction rate $\left(\frac{d\xi}{dt}\right)_{\xi,i}$ and the corresponding temperature $T_{\xi,i}$ for a specific extent of conversion ξ across i temperature programs utilized.[59] Within the present work, E_ξ is calculated for ξ ranging from 0.1 to 0.9 within steps of 0.01. The five temperature programs include heating with constant heating rates β_i of 2, 5, 10, 15, and 20 K/min. For each β_i, the $\left(\frac{d\xi}{dt}\right)_{\xi,i}$ and $T_{\xi,i}$ values are determined. As the term $ln[A_\xi f(\xi)]$ remains constant for a particular value of ξ, the left-hand side of eq 2 depends linearly on the reciprocal temperature. Taking advantage of this linear correlation, the effective E_ξ can be calculated from the slope. Indeed, either isoconversional or model-based fitting approaches can be applied,[60] whereas the latter lacks in consideration of vitrification.[60,61] Still, isoconversional methods provide meaningful insights into mechanistic analysis, detecting governing curing mechanisms, and are essential for detecting the multistep nature of kinetics.[59,60] Therefore, isoconversional methods are applied to first assess the curing reactions of the RTE-DDS formulation.

The activation energies E_ξ (Figure 1a) of RTE-DDS fall between 65 and 50 kJ/mol, which is in the range of conventional epoxy−amine reactions varying from 20 up to 100 kJ/mol.[62−64] The continuous decrease in E_ξ can be attributed to the autocatalytic nature of the system. As indicated in Figure 1b, the change of E_ξ emphasizes that the cross-linking exhibits a more complex behavior and involves multiple reaction mechanisms that require supplementary

https://doi.org/10.1021/acsomega.5c05906
ACS Omega 2025, 10, 49887−49895

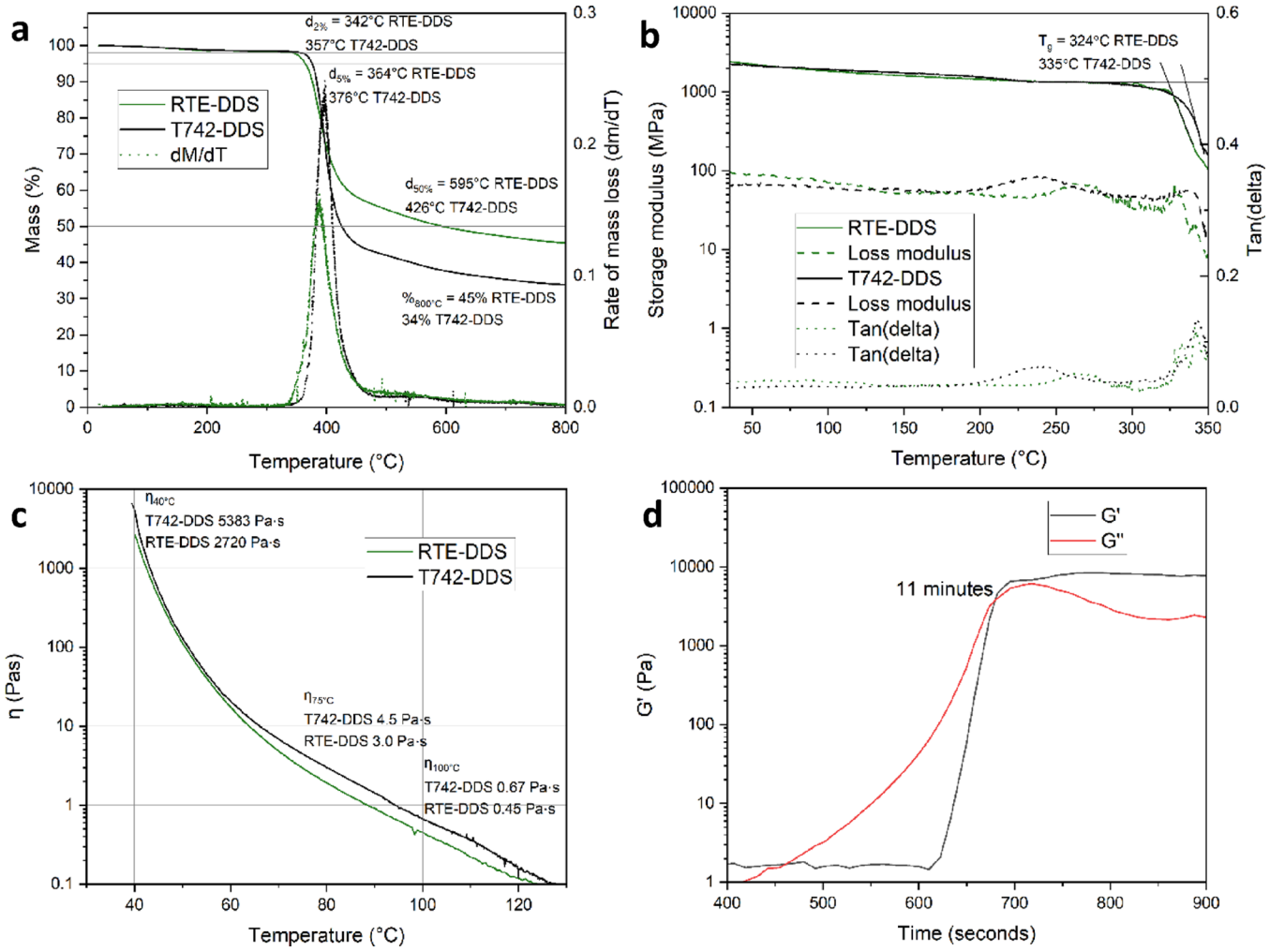

Figure 2. (a) Temperature-dependent viscoelastic properties of RTE-DDS and T742-DDS as measured by DMA. (b) TGA results of RTE-DDS and T742-DDS showcasing the thermal degradation behavior of the resin systems. (c) Viscosity profile of both resins from 40 to 120 °C highlighting the similarities between these resin systems. (d) 180 °C gel point profile of RTE-DDS showing its adequate processing time at this high temperature.

investigation. Therefore, a model-based kinetic model approach is selected to study the reaction kinetics. Model-based approaches are more versatile and able to simulate systems in which temperature history plays a role,[65] which might be relevant to postcuring analysis and combining isothermal dwelling and nonisothermal curing.

Model-Based Kinetics. For the kinetic modeling, the DSC signals are integrated to calculate the evolution of the reaction enthalpy using a linear baseline for dynamic and a strictly horizontal baseline for the isothermal runs. With a final glass transition temperatures $T_{g,\infty}$ greater than 220 °C, at suggested maximum curing temperatures of 160−200 °C, the resin is likely to vitrify once the developing glass transition temperature exceeds the curing temperature. At this point, the reaction process becomes dominated by the diffusion processes in the glassy state (and slows down).

Three dynamic (5, 10, and 15 K/min) (Figure S2) and three isothermal (160, 180, and 200 °C) (Figure 1c) DSC scans were evaluated simultaneously using multivariate analysis to account for isothermal and nonisothermal conditions during curing. Isothermal measurements were included in the fitting routine as these are vital for accurately modeling isothermal cure.[66] The phenomenological Kamal Sourour approach provided the basis for the proposed modeling approach.[67,68] Combining an n^{th} order and an autocatalytic model represented an established approach for the curing behavior of epoxy resins (eq 3):[65,69−71]

$$\frac{d\xi}{dt} = k_1(1-\xi)^{n_1} + k_2\xi^m(1-\xi)^{n_2} \tag{3}$$

Still, T_g is likely to exceed the isothermal curing temperature during the curing process, making the curing reaction diffusion controlled. Therefore, the kinetic constants k_i are superimposed quantities consisting of a chemical $k_{i,\,chem}$ and a diffusion $k_{i,\,diff}$ part (eq 4):

$$\frac{1}{k_i} = \frac{1}{k_{i,chem}} + \frac{1}{k_{i,diff}} \tag{4}$$

while the chemical kinetic constants $k_{i,\,chem}$ exhibit Arrhenius-like behavior (eq 5):

$$k_{i,chem} = A_i e^{-E_i/RT} \tag{5}$$

and the diffusion part kinetic constants $k_{i,\,diff}$ (eq 6):[19]

$$k_{i,diff} = k^*_{i,diff} \cdot e^{(C_1(T-T_g))/(C_2+T-T_g)} \tag{6}$$

https://doi.org/10.1021/acsomega.5c05906
ACS Omega 2025, 10, 49887−49895

Table 1. Physical Properties of RTE-DDS and T742-DDS Resins

resin system	density (kg m^{-3})	T_g(°C)	T_d (°C)	η (Pa·s)	water absorption (% mass increase 14 days submersion)	water contact angle (°)	gel content (%)
RTE-DDS	1307.6 ± 1.67	324[a]	364[b], 595[c]	2720[d], 0.45[e]	1.39 ± 0.04	75.51 ± 2.56	99.96
T742-DDS	1288.9 ± 3.83	335[a]	376[b], 426[c]	5383[d], 0.67[e]	0.97 ± 0.01	71.26 ± 2.98	99.95

[a]Determined by DMA at 3 °C/min heating rate. [b]Temperature at 5% weight loss. [c]Temperature at 50% weight loss. [d]Viscosity at 40 °C. [e]Viscosity at 100 °C.

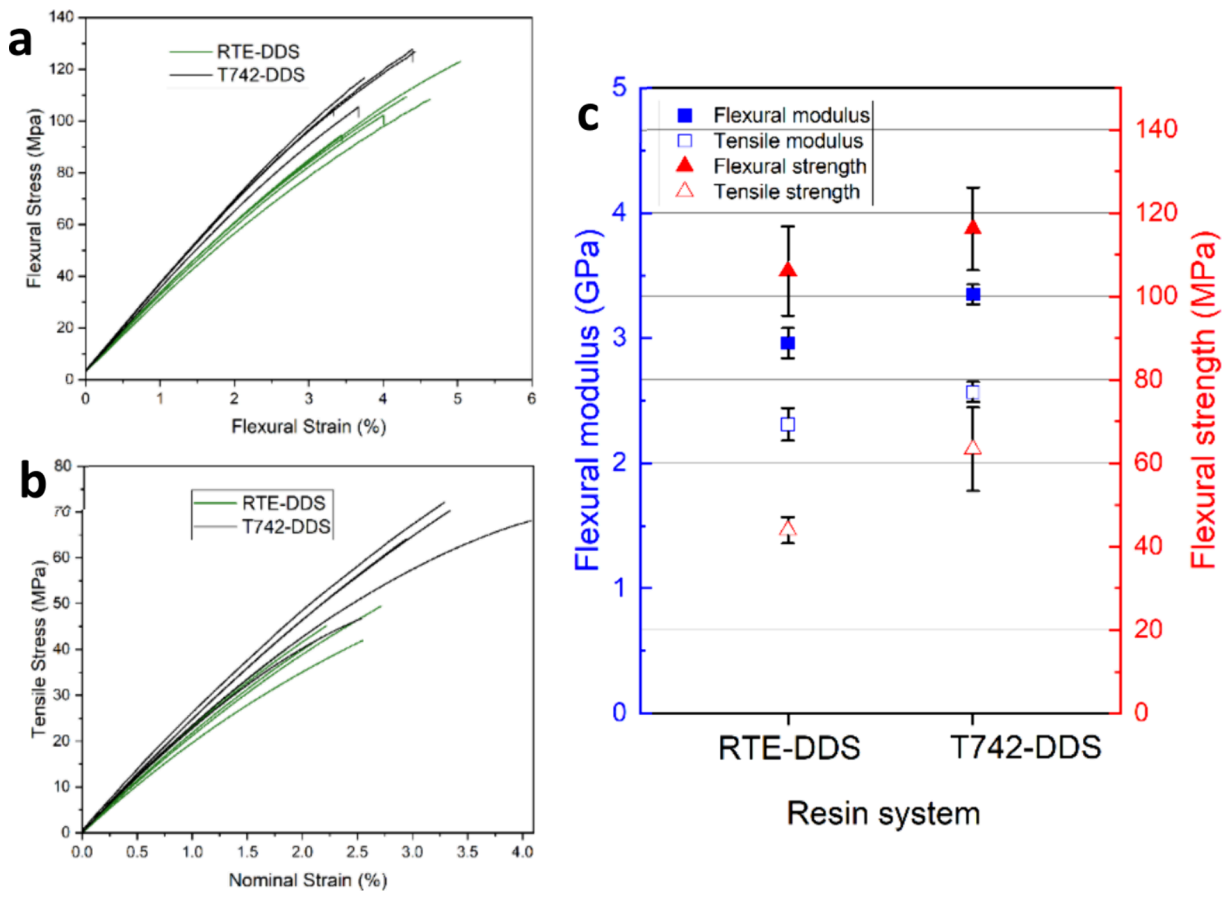

Figure 3. (a) Flexural stress versus strain curves of RTE-DDS and T742-DDS pure resin samples. (b) Tensile stress vs strain curves of RTE-DDS and T742-DDS pure resin samples. (c) Comparison plot of flexural and tensile modulus and strength between RTE-DDS and T742-DDS.

with C_1 and C_2 representing fitting parameters. The correlation between ξ and $T_g(\xi)$ is approximated by the Di-Benedetto-eq (eq 7):[72]

$$\frac{T_g - T_{g,o}}{T_{g,\infty} - T_{g,0}} = \frac{\lambda\xi}{1 - (1-\lambda)\xi}, \; 0 < \lambda < 1 \tag{7}$$

with $T_{g,0}$ representing the initial, $T_{g,\infty}$ the final glass transition temperature, and λ a fitting parameter. In total, the model contains 12 independent material parameters (E_1, E_2, A_1, A_2, m, n_1, n_2, $k^*_{1,\mathrm{diff}}$, $k^*_{2,\mathrm{diff}}$, C_1, C_2, and λ) to describe the curing behavior. The differential equation (eq 3) is solved numerically with the initial condition $\xi = 0$. The model parameters are determined simultaneously for the six data (isothermal and nonisothermal conditions). Isothermal measurements are included in the fitting routine as these are vital for accurately modeling isothermal cure.[66] Even if higher $T_{g,\infty}$ can result from post curing at elevated temperatures above 220 °C, this leads to undesirable side reactions and are not desirable for industrial applications, so that a maximum $T_{g,\infty}$ of 220 °C is defined. Usually, two approaches for determining λ (eq 7) are applied: either λ is determined from the quotient of the change in specific heat capacity in the cured and uncured state[72−74] or from a data set containing i pairings of $T_{g,i}$ and partially cross-linked states ξ_i.[60,75] Unfortunately, it was not suitable to use one of the above methods, as the glass transition during DSC is not very pronounced, which might be attributed to the very high cross-linking density of the resin. Therefore, we include λ as an additional variable in the optimization algorithm and restrict the values within 0.4−0.57[60,73,76] by introducing boundary conditions. Figures S1, S2, and S3 summarize the fitting parameters for the different resin systems. Mean average errors (MAEs) smaller than 2% state an excellent agreement of measurement data and model.

Thermal Properties of the Resin Systems. TGA analysis of the resin systems was performed to understand the maximum service temperature and the degradation behavior of the systems (Figure 2a). Overall, RTE-DDS displayed earlier onset of weight loss in TGA measurements, up to around 400 °C. The $t_{d5\%}$ of RTE-DDS was 342 °C, 15 °C lower than that of T742-DDS. Once the temperature goes

https://doi.org/10.1021/acsomega.5c05906
ACS Omega 2025, 10, 49887−49895

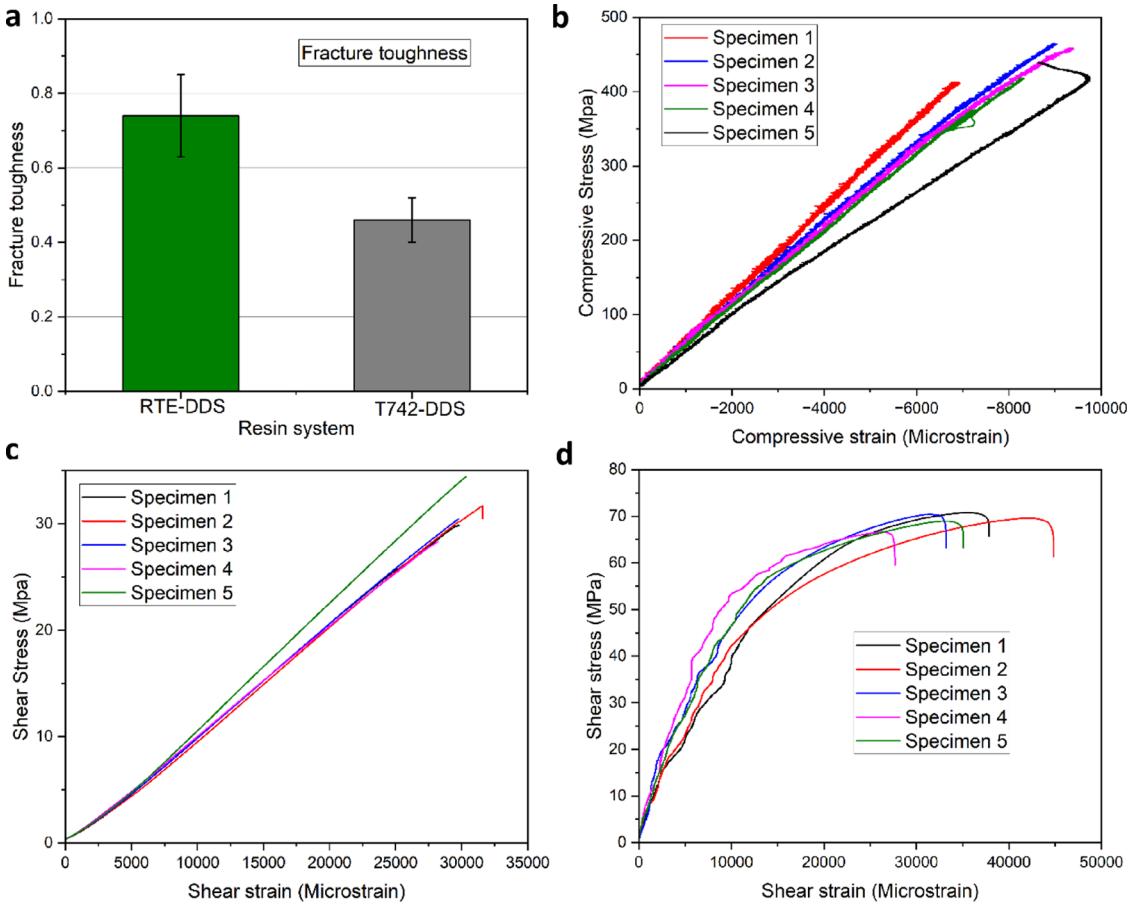

Figure 4. (a) K_{IC} values for RTE-DDS and T742-DDS as determined by SENB coupon testing. (b) CLC compact compression force versus deformation curves for RTE-DDS CFRP. (c) Interlaminar shear strength (ILSS) force vs deformation curves for RTE-DDS CFRP. (d) In-plane shear strength (IPSS) stress versus strain curves for RTE-DDS CFRP.

above 400 °C, the resveratol-based resin degrades slower than the Tactix 742 resin, with $t_{d50\%}$ of 595 °C for RTE-DDS and 426 °C for T742-DDS, 169 °C higher for the biobased system. Similar results have been seen in previous research and highlights the antiflammability potential for Resveratrol-based plastics.[77] Indeed, the final char % at 800 °C was 44.5% for RTE-DDS and 33.3% for T742-DDS, the highest reported char yield for a resveratrol epoxy-based resin system.

Dynamic mechanical analysis (DMA) was performed on the two resin systems (Figure 2b) to evaluate their T_g and any other important material behavior at elevated temperatures, such as decrease in stiffness. The determined T_g for RTE-DDS was 324 °C, comparable to the literature and to the T742-DDS resin with a T_g 11 °C higher. Storage modulus was similar for the two resin formulations at around 2300 MPa at 30 °C, decreasing by half to 1200 MPa at 300 °C. While this difference is significant, the moduli are still within the same order of magnitude, showing that the structural capacity of the resins is still present at this highly elevated temperature. The viscosity profiles (Figure 2c) of the uncured resins show that below 40 °C, the resins are essentially glassy solids. At 40 °C, we see viscosities in the magnitude of kPa s. As the temperature increases, we see a gradual decline in the viscosity of both systems. At 100 °C, the viscosities are below 1 Pa s, making the resins suitable for RTM and VARTM composite manufacturing techniques.[78] Gel point for the RTE-DDS formulation is checked at 180 °C (Figure 2d) to ensure adequate processing time for CFRP manufacturing and comes out at 11 min. Industry standard formulation RTM6 has gel point of around 30 min at 180 °C according to the Hexcel technical data sheet, showing RTE-DDS reacts considerably faster.

Physical Properties. Alongside the kinetic and thermal evaluation of the resin systems, physical tests were carried out to compare the properties of the bulk materials. A full collection of these physical properties can be found in Table 1. Density was determined according to ASTM D792 and revealed comparable densities of the two resins, with RTE-DDS having a slightly higher density. Water contact angle was used to assess the hydrophilicity of materials. Both RTE-DDS and T742-DDS showed hydrophilic behavior (<90°) with RTE-DDS being slightly less hydrophilic than T742-DDS. Water absorption was a critical consideration for epoxy−amine formulations as water acts as a plasticizer, considerably decreasing stiffness and T_g of materials. ASTM D570 was used to determine the water absorption of the materials (Table 1). After 2 weeks of immersion in water, the RTE-DDS mass increased by 1.39% on average, with T742-DDS increasing by 0.97% in the same time frame. Gel content determined according to ASTM D2765 showed a high gel fraction for both formulations.

Mechanical Properties. The mechanical properties of bulk resin material give essential information when considering its suitability for CFRP manufacturing. Flexural, tensile, and fracture toughness were evaluated according to ASTM standards D790, D638, and D5045, respectively. Detailed

https://doi.org/10.1021/acsomega.5c05906
ACS Omega 2025, 10, 49887−49895

Table 2. Bulk Material Properties of Pure Resin Systems

resin system	flexural modulus (GPa)	flexural strength (MPa)	tensile modulus (GPa)	tensile strength (MPa)	fracture toughness (mpa $m^{0.5}$)
RTE-DDS	2.96 ± 0.12	106.10 ± 10.70	2.31 ± 0.13	43.97 ± 3.12	0.74 ± 0.11
T742-DDS	3.35 ± 0.08	116.18 ± 9.91	2.57 ± 0.08	63.36 ± 10.02	0.46 ± 0.06

sample preparation, test procedure, and results can be found in Supporting Information. Flexural testing revealed a flexural modulus of 2.96 GPa and a flexural strength of 106.10 MPa for the RTE-DDS resin (Figure 3a). This was slightly lower than the values of 3.35 GPa and 116.18 MPa determined for T742-DDS. Tensile results showed T742-DDS has a slightly higher modulus and significantly higher strength (44%). RTE-DDS showed tensile modulus and strength of 2.31 and 43.97 GPa compared to T742-DDS at 2.57 and 63.36 MPa (Figure 3b), still with significantly smaller failure stresses of 2.3% ± 0.3 for RTE-DDS and 3.3 ± 0.5 for T742-DDS. These results show that the resveratrol epoxy monomer forms a slightly weaker and less stiff material than Tactix 742. Mode I fracture toughness testing through SENB samples then showed expected results, with RTE-DDS showing a higher value of 0.74 MPa $m^{0.5}$ compared to T742-DDS's value of 0.46 MPa $m^{0.5}$ (Figure 4a). While modulus and strength were between 11 and 13% and 10−44% lower for RTE-DDS, the fracture toughness value was 61% higher than that of T742-DDS, which aligned with current understanding of free volume theory in thermoset materials.[79−81] Bulk properties are comparatively summarized in Table 2.

CFRP Manufacturing and Testing Results. CFRP samples in three geometries were manufactured with RTE-DDS matrix using the vacuum bagging and autoclave curing technique. The detailed procedure can be found in Supporting Information. The fiber volume and void content of the manufactured composite material were evaluated using ASTM D3171.

Fiber volume came out at 37% ± 2.7, slightly low for high-performance composites due to the high viscosity of the formulation and the available vacuum bagging and autoclave manufacturing technique. Coupled with a void content of 0.55% ± 0.26, these two composite components were acceptable for the following composite tests. ILSS was determined at 30.6 MPa ± 1.5. IPSS was 70.4 MPa ± 0.87. In-plane shear modulus was 4.45 GPa ± 0.66. Combined loading compression (CLC) test revealed a compressive strength of 438.6 MPa ± 20.6. Compressive modulus was 58.7 ± 2.9 GPa ± 2.9.

CONCLUSIONS

In this research, resveratrol triglycidyl ether epoxy monomer with 4,4-diaminodiphenylsulfone amine hardener formulation has been characterized across its reactivity and processing domain, with in-depth DSC studied and CFRP sample manufacturing being showcased. Furthermore, the RTE-DDS resin was shown to perform at a comparative level against the analogous Tactix 742 resin system in the mechanical and physical property domains. The resins differed most in their thermal properties and fracture toughness values. RTE-DDS displayed a slightly earlier onset of degradation compared to T742-DDS, but displayed a higher char yield at 800 °C, which showed its potential in high-heat zone applications such as those used for Tactix 742. In flexural and tensile testing, the resins behaved similar; however, the T742-DDS formulation did show generally higher strengths and moduli. The K_{IC} value for RTE-DDS was 61% higher than the T742-DDS resin at 0.74 mpa $m^{0.5}$. These results build upon existing research to highlight the potential of biobased resin systems in replacing existing high-performance petro-based systems.

ASSOCIATED CONTENT

Supporting Information

The Supporting Information is available free of charge at https://pubs.acs.org/doi/10.1021/acsomega.5c05906.

Details on sample preparation and mechanical tests, cure kinetics studies, formulations used to calculate mechanical properties, tables delineating specimen properties for mechanical tests (PDF)

AUTHOR INFORMATION

Corresponding Author

Baris Kumru − *Aerospace Structures & Materials Department, Faculty of Aerospace Engineering, Delft University of Technology, Delft 2629 HS, The Netherlands*; orcid.org/0000-0002-1203-4019; Email: b.kumru@tudelft.nl

Authors

William E. Dyer − *Aerospace Structures & Materials Department, Faculty of Aerospace Engineering, Delft University of Technology, Delft 2629 HS, The Netherlands*

Elmar-Daniel Alasoo − *Aerospace Structures & Materials Department, Faculty of Aerospace Engineering, Delft University of Technology, Delft 2629 HS, The Netherlands*

Niklas Lorenz − *Aerospace Structures & Materials Department, Faculty of Aerospace Engineering, Delft University of Technology, Delft 2629 HS, The Netherlands*; orcid.org/0000-0003-1275-2579

Complete contact information is available at: https://pubs.acs.org/10.1021/acsomega.5c05906

Author Contributions

[†]William E. Dyer and Elmar-Daniel Alasoo contributed equally.

Notes

The authors declare no competing financial interest.

ACKNOWLEDGMENTS

The authors acknowledge valuable support from ASM department and DASML technical staff. We acknowledge that this article is made possible through funding provided by NXTGEN HIGHTECH 01 Composite Focus Area.

REFERENCES

(1) Pascault, J. P.; Williams, R. J. J. General Concepts about Epoxy Polymers. In *Epoxy Polymers: New Materials and Innovations*; Wiley-VCH Verlag GmbH & Co. 2010. pp 1−12, .

(2) Moghaddam, A.; Kumru, B.; Bergsma, O. K. Recyclable twin matrix composites. *Compos. Commun.* **2024**, *50*, No. 102010.

(3) Pham, H. Q.; Marks, M. J. Epoxy Resins. In *Ullmann's Encyclopedia of Industrial Chemistry*. Wiley-VCH Verlag GmbH & Co. 2005. .

(4) Negoita, C.; Cristache, N.; Bodor, M. The Epoxy Resin - History and Perspectives. *Mater. Plast.* **2016**, *53*, 564.
(5) Apostolidis, D.; Dyer, W. E.; Dransfeld, C. A.; Kumru, B. An algae-derived partially renewable epoxy resin formulation for glass fibre-reinforced sustainable polymer composites. *RSC Appl. Polym.* **2024**, *2*, 149−154.
(6) Zhao, S.; Liu, Q.; Yuan, A.; Liu, Z.; Zhou, S.; Fu, X.; Lei, J.; Jiang, L. Intrinsic toughened conductive thermosetting epoxy resins: utilizing dynamic bond and electrical conductivity to access electric and thermal dual-driven shape memory. *Mater. Chem. Front.* **2022**, *6*, 1989−1999.
(7) Ghosh, S.; Manna, R. Epoxy-based polymer bearing triphenylamine units: a highly selective fluorescent chemosensor for Hg2+ ions. *RSC Adv.* **2014**, *4*, 5798−5802.
(8) Schlack, Paul, *"Manufacture of amines of high molecular weight, which are rich in nitrogen"*. German Patent 676117, 1938.
(9) Aghadavoudi, F.; Golestanian, H.; Tadi Beni, Y. Investigating the effects of resin crosslinking ratio on mechanical properties of epoxy-based nanocomposites using molecular dynamics. *Polym. Compos.* **2017**, *38*, E433−E442.
(10) Tu, J.; Moran, V. J.; Rooney, E. E.; Palmese, G. R.; Stanzione, J. F. A study on the effects of network interconnection on the topological, physical, thermomechanical, and mechanical properties of epoxy-methacrylate interpenetrating polymer networks. *Polymer* **2024**, *304*, No. 127130.
(11) FernandezNograro, F.; Valea, A.; LlanoPonte, R.; Mondragon, I. Dynamic and mechanical properties of DGEBA/poly(propylene oxide) amine based epoxy resins as a function of stoichiometry. *Eur. Polym. J.* **1996**, *32*, 257−266.
(12) Lee, J. Y.; Jang, J. IR study of hydrogen bonding in novel liquid crystalline epoxy/DGEBA blends. *Polym. Bull.* **1997**, *38*, 439−445.
(13) Mora, A. S.; Tayouo, R.; Boutevin, B.; David, G.; Caillol, S. A perspective approach on the amine reactivity and the hydrogen bonds effect on epoxy-amine systems. *Eur. Polym. J.* **2020**, *123*, No. 109460.
(14) Abdulrazack, N. The Effect of Various Hardeners on the Mechanical and Thermal Properties of Epoxy Resin. *Int. J. Eng. Res. Technol.* **2014**, *3*, 2662−2665.
(15) Drzal, L. T.; Madhukar, M. Fibre-matrix adhesion and its relationship to composite mechanical properties. *J. Mater. Sci.* **1993**, *28*, 569−610.
(16) Rajak, D. K.; Wagh, P. H.; Linul, E. Manufacturing Technologies of Carbon/Glass Fiber-Reinforced Polymer Composites and Their Properties: A Review. *Polymers* **2021**, *13*, 3721.
(17) Ekuase, O. A.; Anjum, N.; Eze, V. O.; Okoli, O. I. A Review on the Out-of-Autoclave Process for Composite Manufacturing. *J. Compos. Sci.* **2022**, 172.
(18) Marchetti, M.; Laurenzi, S. *Composites and Their Properties*, ed. Hu, N. IntechOpen: Rijeka, 2012, .
(19) Naik, T. P.; Singh, I.; Sharma, A. K. Processing of polymer matrix composites using microwave energy: A review. *Compos. Part A-Appl. S.* **2022**, *156*, No. 106870.
(20) Thomas, J.; Patil, R. S.; Patil, M.; John, J. Addressing the Sustainability Conundrums and Challenges within the Polymer Value Chain. *Sustainability* **2023**, *15*, 15758.
(21) Vieyra, H.; Molina-Romero, J. M.; Calderón-Nájera, J. D.; Santana-Díaz, A. Engineering, Recyclable, and Biodegradable Plastics in the Automotive Industry: A Review. *Polymers* **2022**, *14*, 3412.
(22) Haq, F.; Kiran, M.; Khan, I. A.; Mehmood, S.; Aziz, T.; Haroon, M. Exploring the pathways to sustainability: A comprehensive review of biodegradable plastics in the circular economy. *Mater. Today Sustain.* **2025**, *29*, No. 101067.
(23) Brooks, A. L.; Havas, V. Strengthening global plastic policy with systems analysis. *Nat. Sustain.* **2025**, *8*, 714−723.
(24) Yaghoubi, V.; Kumru, B. Retrosynthetic life cycle assessment: a short perspective on the sustainability of integrating thermoplastics and artificial intelligence into composite systems. *Adv. Sust. Syst.* **2024**, *8*, 2300543.
(25) Wang, Z.; Ganewatta, M. S.; Tang, C. Sustainable polymers from biomass: bridging chemistry with materials and processing. *Prog. Polym. Sci.* **2020**, *101*, No. 101197.
(26) Dyer, W. E.; Kumru, B. Polymers as Aerospace Structural Components: How to Reach Sustainability? *Macromol. Chem. Phys.* **2023**, *224*, 2300186.
(27) Hatti-Kaul, R.; Nilsson, L. J.; Zhang, B. Z.; Rehnberg, N.; Lundmark, S. Designing Biobased Recyclable Polymers for Plastics. *Trends Biotechnol.* **2020**, *38*, 50−67.
(28) López-Gómez, J. P.; Pérez-Rivero, C.; Venus, J. Valorisation of solid biowastes: The lactic acid alternative. *Process Biochem.* **2020**, *99*, 222−235.
(29) Morgan, R. J. *Epoxy Resins and Composites I*; Springer, 1985, 72.
(30) Sheldon, R. A. Green and sustainable manufacture of chemicals from biomass: state of the art. *Green Chem.* **2014**, *16*, 950−963.
(31) Booker, J. L.Cellulose Chemistry and Technology. 1989, *23*, 2326.
(32) Kaur, B.; Chakraborty, D. Biotechnological and molecular approaches for vanillin production: a review. *Appl. Biochem. Biotechnol.* **2013**, *169*, 1353−1372.
(33) Fache, M.; Darroman, E.; Besse, V.; Auvergne, R.; Caillol, S.; Boutevin, B. Vanillin, a promising biobased building-block for monomer synthesis. *Green Chem.* **2014**, *16*, 1987−1998.
(34) Jia, Y.; Zhang, Y.; Meng, F.; Chen, Z.; Fei, H.; Zhou, D.; Zhu, M.; Yuan, X. *Polymers* **2025**, *17*, 94.
(35) Joul, P.; Ho, T. T.; Kallavus, U.; Konist, A.; Leiman, K.; Salm, O. S.; Kulp, M.; Koel, M.; Lukk, T. Characterization of Organosolv Lignins and Their Application in the Preparation of Aerogels. *Materials* **2022**, *15*, 2861.
(36) Fu, B.; Xiao, G.; Zhang, Y.; Yuan, J. One-Pot Bioconversion of Lignin-Derived Substrates into Gallic Acid. *J. Agric. Food Chem.* **2021**, *69*, 11336−11341.
(37) Kim, H.; Rencoret, J.; Elder, T. J.; del Rio, J. C.; Ralph, J. Biomimetic oxidative copolymerization of hydroxystilbenes and monolignols. *Sci. Adv.* **2023**, 9.
(38) Dinu, R.; Lafont, U.; Damiano, O.; Mija, A. High Glass Transition Materials from Sustainable Epoxy Resins with Potential Applications in the Aerospace and Space Sectors. *ACS Appl. Polym. Mater.* **2022**, *4*, 3636−3646.
(39) Dinu, R.; Lafont, U.; Damiano, O.; Mija, A. Sustainable and recyclable thermosets with performances for high technology sectors. An environmental friendly alternative to toxic derivatives. *Front. Mater.* **2023**, 10.
(40) Meng, L.; Diao, M.; Wang, Q.; Peng, L.; Li, J.; Xie, N. Efficient biosynthesis of resveratrol via combining phenylalanine and tyrosine pathways in Saccharomyces cerevisiae. *Microb. Cell Fact.* **2023**, *22*, 46.
(41) Lu, H.; Sun, S. D.; Bi, Y. L.; Yang, G. L.; Ma, R. L.; Yang, H. F. Enzymatic epoxidation of soybean oil methyl esters in the presence of free fatty acids. *Eur. J. Lipid Sci. Technol.* **2010**, *112*, 1101−1105.
(42) Shoda, S.; Uyama, H.; Kadokawa, J.; Kimura, S.; Kobayashi, S. Enzymes as Green Catalysts for Precision Macromolecular Synthesis. *Chem. Rev.* **2016**, *116*, 2307−2413.
(43) Qian, Z.; Xiao, Y.; Zhang, X.; Li, Q.; Wang, L.; Fu, F.; Diao, H.; Liu, X. Bio-based epoxy resins derived from diphenolic acid via amidation showing enhanced performance and unexpected autocatalytic effect on curing. *Chem. Eng. J.* **2022**, No. 135022.
(44) Li, P.; Ma, S.; Wang, B.; Xu, X.; Feng, H.; Yu, Z.; Yu, T.; Liu, Y.; Zhu, J. Degradable Benzyl Cyclic Acetal Epoxy Monomers with Low Viscosity: Synthesis, Structure-Property Relationships, Application in Recyclable Carbon Fiber Composite. *Compos. Sci. Technol.* **2022**, *219*, No. 109243.
(45) Yang, W. J.; Ding, H.; Puglia, D.; Kenny, J. M.; Liu, T. X.; Guo, J. Q.; Wang, Q. W.; Ou, R. X.; Xu, P. W.; Ma, P. M.; Lemstra, P. J. Bio-renewable polymers based on lignin-derived phenol monomers: Synthesis, applications, and perspectives. *SUSMAT* **2022**, *2*, 535−568.
(46) Ge, M. Y.; Liang, G. Z.; Gu, A. A facile strategy and mechanism to achieve biobased bismaleimide resins with high thermal-resistance and strength through copolymerizing with unique propargyl ether-

https://doi.org/10.1021/acsomega.5c05906
ACS Omega 2025, 10, 49887−49895

functionalized allyl compound. *React. Funct. Polym.* **2023**, *186*, No. 105570.
(47) Dyer, W. E.; Gupta, P.; Dransfeld, C. A.; Lorenz, N.; Kumru, B. Formulating Brown Algae Derived Phloroglucinol-Based Epoxy Resin for High Performance Applications. *ACS Appl. Polym. Mater.* **2024**, *6*, 13371−13377.
(48) Lorenz, N.; Dyer, W. E.; Kumru, B. High-Performance Vitrimer Entailing Renewable Plasticizer Engineered for Processability and Reactivity toward Composite Applications. *ACS Appl. Polym. Mater.* **2025**, *7*, 1934−1946.
(49) Cash, J. J.; Davis, M. C.; Ford, M. D.; Groshens, T. J.; Guenthner, A. J.; Harvey, B. G.; Lamison, K. R.; Mabry, J. M.; Meylemans, H. A.; Reams, J. T.; Sahagun, C. M. High Tg thermosetting resins from resveratrol. *Polym. Chem.* **2013**, *4*, 3859−3865.
(50) Cambrea, L. R.; Davis, M. C.; Garrison, M. D.; Groshens, T. J.; Lyon, R. E.; Safronava, N. Processable cyanate ester resin from Cis resveratrol. *J. Polym. Sci., Polym. Chem.* **2017**, *55*, 971−980.
(51) Tian, Y.; Wang, Q.; Shen, L.; Cui, Z.; Kou, L.; Cheng, J.; Zhang, J. A renewable resveratrol-based epoxy resin with high Tg, excellent mechanical properties and low flammability. *Chem. Eng. J.* **2020**, *383*, No. 123124.
(52) Tian, Y.; Ke, M.; Wang, X.; Wu, G.; Zhang, J.; Cheng, J. A resveratrol-based epoxy resin with ultrahigh Tg and good processability. *Eur. Polym. J.* **2021**, *147*, No. 110282.
(53) Shang, L.; Zhang, X. P.; Zhang, M. J.; Jin, L.; Liu, L.; Xiao, L. H.; Li, M.; Ao, Y. H. A highly active bio-based epoxy resin with multifunctional group: synthesis, characterization, curing and properties. *J. Mater. Sci.* **2018**, *53*, 5402−5417.
(54) Garrison, M. D.; Harvey, B. G. Structure-property relationships of cis-resveratrol cyanate ester blends. *Polymer* **2021**, *213*, No. 123194.
(55) Huang, G.; Fang, L. X.; Wang, C. Y.; Dai, M. L.; Sun, J.; Fang, Q. A bio-based low dielectric material at a high frequency derived from resveratrol. *Polym. Chem.* **2021**, *12*, 402−407.
(56) Vyazovkin, S. *Isoconversional Kinetics of Thermally Stimulated Processes*; Springer International Publishing, 2015.
(57) Vyazovkin, S.; Burnham, A. K.; Criado, J. M.; Pérez-Maqueda, L. A.; Popescu, C.; Sbirrazzuoli, N. ICTAC Kinetics Committee recommendations for performing kinetic computations on thermal analysis data. *Thermochim. Acta* **2011**, *520*, 1−19.
(58) Friedman, H. L. Kinetics of thermal degradation of char-forming plastics from thermogravimetry. Application to a phenolic plastic. *J. Polym. Sci., Polym. Symp.* **1964**, *6*, 183−195.
(59) Sbirrazzuoli, N. Determination of pre-exponential factors and of the mathematical functions f(α) or G(α) that describe the reaction mechanism in a model-free way. *Thermochim. Acta* **2013**, *564*, 59−69.
(60) Tziamtzi, C. K.; Chrissafis, K. Optimization of a commercial epoxy curing cycle via DSC data kinetics modelling and TTT plot construction. *Polymer* **2021**, *230*, No. 124091.
(61) Stanko, M.; Stommel, M. Kinetic Prediction of Fast Curing Polyurethane Resins by Model-Free Isoconversional Methods. *Polymers* **2018**, *10*, 698.
(62) Cai, H.; Li, P.; Sui, G.; Yu, Y.; Li, G.; Yang, X.; Ryu, S. Curing kinetics study of epoxy resin/flexible amine toughness systems by dynamic and isothermal DSC. *Thermochim. Acta* **2008**, *473*, 101−105.
(63) Vyazovkin, S.; Sbirrazzuoli, N. Mechanism and Kinetics of Epoxy−Amine Cure Studied by Differential Scanning Calorimetry. *Macromolecules* **1996**, *29*, 1867−1873.
(64) Demleitner, M.; Sanchez-Vazquez, S. A.; Raps, D.; Bakis, G.; Pflock, T.; Chaloupka, A.; Schmölzer, S.; Altstädt, V. Dielectric analysis monitoring of thermoset curing with ionic liquids: From modeling to the prediction in the resin transfer molding process. *Polym. Compos.* **2019**, *40*, 4500−4509.
(65) Skordos, A.; Partridge, I. Cure kinetics modeling of epoxy resins using a non-parametric numerical procedure. *Polym. Eng. Sci.* **2001**, *41*, 793−805.
(66) Bernath, A.; Karger, L.; Henning, F. Accurate Cure Modeling for Isothermal Processing of Fast Curing Epoxy Resins. *Polymers* **2016**, *8*, 390.
(67) Lahlali, D.; Naffakh, M.; Dumon, M. Cure kinetics and modeling of an epoxy resin cross-linked in the presence of two different diamine hardeners. *Polym. Eng. Sci.* **2005**, *45*, 1581−1589.
(68) Sourour, S.; Kamal, M. R. Differential scanning calorimetry of epoxy cure: isothermal cure kinetics. *Thermochim. Acta* **1976**, *14*, 41−59.
(69) Navabpour, P.; Nesbitt, A.; Degamber, B.; Fernando, G.; Mann, T.; Day, R. Comparison of the curing kinetics of the RTM6 epoxy resin system using differential scanning calorimetry and a microwave-heated calorimeter. *J. Appl. Polym. Sci.* **2006**, *99*, 3658−3668.
(70) Karkanas, P. I.; Partridge, I. K. J. Cure modeling and monitoring of epoxy/amine resin systems. I. Cure kinetics modeling. *J. Appl. Polym. Sci.* **2000**, *77*, 1419−1431.
(71) Karkanas, P. I.; Partridge, I. K.; Attwood, D. Modelling the cure of a commercial epoxy resin for application in resin transfer moulding. *Polym. Int.* **1996**, *41*, 183−191.
(72) Pascault, J. P.; Williams, R. J. J. Glass transition temperature versus conversion relationships for thermosetting polymers. *J. Polym. Sci., Part B:Polym. Phys.* **1990**, *28*, 85−95.
(73) Strasser, C.; Moukhina, E.; Hartmann, J. Time−Temperature-Transformation (TTT) Cure Diagram of an Epoxy-Amine System. *Macromol. Theory Simul.* **2024**, *33*, 2400039.
(74) Causse, N.; Benchimol, S.; Martineau, L.; Carponcin, D.; Lonjon, A.; Fogel, M.; Dandurand, J.; Dantras, E.; Lacabanne, C. Polymerization study and rheological behavior of a RTM6 epoxy resin system during preprocessing step. *J. Therm. Anal. Calorim.* **2015**, *119*, 329−336.
(75) Lorenz, N.; Müller-Pabel, M.; Gerritzen, J.; Müller, J.; Gröger, B.; Schneider, D.; Fischer, K.; Gude, M.; Hopmann, C. Characterization and modeling cure- and pressure-dependent thermo-mechanical and shrinkage behavior of fast curing epoxy resins. *Polym. Test.* **2022**, *108*, No. 107498.
(76) Wise, C. W.; Cook, W. D.; Goodwin, A. A. Chemico-diffusion kinetics of model epoxy-amine resins. *Polymer* **1997**, *38*, 3251−3261.
(77) Tian, Y.; Wang, Q.; Shen, L.; Cui, Z.; Kou, L.; Cheng, J.; Zhang, J. A renewable resveratrol-based epoxy resin with high Tg, excellent mechanical properties and low flammability. *Chem. Eng. J.* **2020**, *383*, No. 123124.
(78) Gajjar, T.; Shah, D. B.; Joshi, S. J.; Patel, K. M. Analysis of Process Parameters for Composites Manufacturing using Vacuum Infusion Process. *Mater. Today Proc.* **2020**, *21*, 1244−1249.
(79) Dyer, W. E.; Schut, H.; Dransfeld, C. A.; Kumru, B.Bio-Based Epoxies: Mechanical Properties And Free Volume Perspectives. *Proceedings of the 21st European Conference on Composite Materials*; European Society for Composite Materials (ESCM) and the Ecole Centrale de Nantes 2024, *1*, 137143.
(80) Jean, Y. C.; Deng, Q.; Nguyen, T. T. Free-Volume Hole Properties in Thermosetting Plastics Probed by Positron Annihilation Spectroscopy: Chain Extension Chemistry. *Macromolecules* **1995**, *28*, 8840−8844.
(81) Li, C.; Strachan, A. Free volume evolution in the process of epoxy curing and its effect on mechanical properties. *Polymer* **2016**, *97*, 456−464.

https://doi.org/10.1021/acsomega.5c05906
ACS Omega 2025, 10, 49887−49895